

Local structure study about Co in $\text{YBa}_2(\text{Cu}_{1-x}\text{Co}_x)_3\text{O}_{7-\delta}$ thin films using polarized XAFS

E. D. Bauer, F. Bridges, C. H. Booth
Physics Department, University of California, Santa Cruz, CA 95064

J. B. Boyce
Xerox Palo Alto Research Center, Palo Alto, CA 94304

T. Claeson, G. Brorsson
Physics Department, Chalmers Univ. of Tech., S-41296 Gothenburg, Sweden

Y. Suzuki
AT&T Bell Laboratories, Murray Hill, NJ 07974
(Draft: April 1, 2018)

We have studied the local structure around Co in $\text{YBa}_2(\text{Cu}_{1-x}\text{Co}_x)_3\text{O}_{7-\delta}$ thin films with three different concentrations: $x=0.07, 0.10, 0.17$, and in a $\text{PrBa}_2(\text{Cu}_{1-x}\text{Co}_x)_3\text{O}_{7-\delta}$ thin film of concentration $x=0.05$ using the X-ray Absorption Fine Structure (XAFS) technique. Data were collected at the Co K -edge with polarizations both parallel and perpendicular to the film surface. We find that the oxygen neighbors are well ordered and shortened in comparison with YBCO Cu-O values to 1.80 \AA and 1.87 \AA in the c -axis and ab -plane, respectively. A comparison of further neighbors in the thin film and powder data show that these peaks in the film are suppressed in amplitude relative to the powder samples, which suggests there is more disorder and/or distortions of the Co environment present in the thin films.

PACS numbers: 61.10.Ht, 78.70.Dm, 74.72.Jt, 74.72.Bk

I. INTRODUCTION

The substitution of different cations for copper in $\text{YBa}_2\text{Cu}_3\text{O}_{7-\delta}$ (YBCO) has been widely used to study the relationship between the crystal structure and superconductivity, particularly the differences between Cu(2) in the CuO_2 planes and Cu(1) in the CuO “chains” (See Fig. 1 for the crystal structure). Previous investigations have shown that Co, Al, and Fe substitute primarily on the Cu(1) site at low defect concentrations¹⁻³, and thereby provide a probe to study the effect of the Cu(1) chains on the superconducting properties. Co and Fe both suppress the superconducting transition temperature, T_c , to zero at roughly 15% substitution in bulk samples^{4,5}. However, the actual value of T_c in a given sample depends strongly on the sample preparation. (For example we showed earlier that T_c of 10% YBCO:Fe thin film samples could vary from ~ 0 -80 K depending on the deposition temperature and cool-down rate⁶.) It has also been observed⁷⁻⁹ that adding Co (or Fe) to YBCO increases the O concentration.

Many experimental reports indicate that the local environment about Co is strongly distorted or disordered. Mössbauer experiments suggest that there are 3-4 inequivalent sites for Fe (Co should be similar) with different O coordinations¹⁰. X-ray Absorption Fine Structure (XAFS) experiments show that the first neighbor oxygens are quite well ordered but the further neighbor environment is distorted^{1,9,11}. Several groups have interpreted their data in terms of chain-like Co clusters in the Cu(1) layer^{4,12} and in some cases a $\langle 110 \rangle$ off-center displacement of some of the Co atoms^{1,11,13}. These small clusters are thought to be responsible for the suppression of T_c by distorting the Cu planes or by removing holes from the superconducting layer. Each of these reports has a different proposal for the local structure, again suggesting that it is heavily dependent on sample preparation. There is also the question¹⁴ as to whether all the Co is actually in the bulk YBCO – is some Co located in grain boundaries or within other small crystallites?

Recent interest in Co substituted YBCO (YBCO:Co) has arisen in conjunction with developments in SNS (Superconducting-Normal-Superconducting) junctions. In these junctions it is highly desirable for the normal metal to have the same thermal expansion and lattice parameters as YBCO. YBCO:Co is nearly ideal in this respect and produces junctions with the lowest resistance¹⁵⁻¹⁷. Despite the enthusiasm for these devices and the finding that YBCO:Co makes a good normal conductor for the junctions, there have been only been a few investigations involving YBCO:Co thin films¹⁵⁻¹⁸. Previous studies of Co substituted YBCO have been on powder samples for which the relative contributions of the various peaks in the XAFS r -space plots are different than in polarized XAFS studies.

In this paper, we present a polarized XAFS study of the local structure around the Co ions in thin films of $\text{YBa}_2(\text{Cu}_{1-x}\text{Co}_x)_3\text{O}_{7-\delta}$. Three Co concentrations were used: $x=0.07, 0.10, 0.17$, and the T_c 's were similar to bulk material. We find that the nearest neighbor oxygen atoms about the Co are contracted both along the c -axis and in the ab -plane. In previous XAFS measurements¹ on powder samples, an average contraction was thought to be primarily a result of an ab -plane contraction. We also studied a $\text{PrBa}_2(\text{Cu}_{1-x}\text{Co}_x)_3\text{O}_{7-\delta}$ (PBCO:Co) thin film sample with a Co concentration of $x=0.05$ and $T_c = 0$, to see if any significant change occurred in the Co environment when Y is replaced by Pr.

A brief introduction to polarized XAFS is presented in Sec. II. In Sec. III we give some experimental details and then outline the general features of the data, including a comparison with powder data in Sec. IV. A discussion of theoretical simulations for various Co distortions is contained in Sec. V. We describe our fits in Sec. VI and discuss our conclusions in Sec. VII.

II. POLARIZED XAFS

The standard XAFS equation for a polycrystalline sample can be written as:

$$k\chi(k) = \sum_j \frac{A_j(k)}{R_j^2} \sin[2kR_j + \phi_j(k)] \exp(-2k^2\sigma_j^2 - 2R_j/\lambda(k)) \quad (1)$$

where the sum is taken over the shells of atoms at a distance R_j from the absorbing atom, with amplitude A_j , k is the k -vector of the ejected photon ($k = [2m(E - E_o)]^{1/2}/\hbar$ where E is the photon energy, E_o is the edge energy), $\phi_j(k)$ is the total phase shift of the photoelectron due to its interaction with the back scattering and absorbing atoms, λ is the electron mean free path, and σ_j (Debye-Waller factor) is the mean variation of R_j arising from static and thermal disorder. The amplitude is given by:

$$A_j = N_j S_0^2 F(R_j, k)$$

in which N_j is the number of like atoms at a distance R_j , S_0^2 is an overall reduction factor accounting for shake-up and shake-off processes, and $F(R_j, k)$ is the scattering amplitude. The XAFS technique and data analysis process have been described in detail elsewhere (for example, see Ref. 19,20).

In the absorption process the outgoing electron is preferentially ejected along the x-ray polarization vector, $\hat{\mathbf{P}}$, and the outgoing electron intensity distribution varies as $\cos^2(\theta) = (\hat{\mathbf{R}} \cdot \hat{\mathbf{P}})^2$ where $\hat{\mathbf{R}}$ is in the direction of the ejected electron. Consequently, for non-cubic materials one can take advantage of the high degree of polarization of synchrotron radiation by using an oriented sample, usually a single crystal or oriented thin film. Neighboring atoms along the polarization direction are preferentially probed while atoms located in a plane perpendicular to $\hat{\mathbf{P}}$ are not observed. Using polarized XAFS in the context of YBCO:Co has the advantage of minimizing the contributions from the in-plane O(1) atoms with the x-ray polarization along the c -axis of the film (i.e. normal to the film); conversely, when the polarization vector is in the ab -plane, the contribution from the axial oxygen O(4) atoms is negligible.

III. EXPERIMENTAL DETAILS

The YBCO:Co films were made by pulsed laser deposition onto SrTiO_3 substrates and are estimated to be 3000 Å thick. Transition temperatures for the three concentrations of Co in $\text{YBa}_2(\text{Cu}_{1-x}\text{Co}_x)_3\text{O}_{7-\delta}$ are: 38 K for $x=0.07$, 42 K for $x=0.10$, and nonsuperconducting for $x=0.17$. The PBCO:Co sample was prepared by laser ablation on a LaAlO_3 substrate and is 5000 Å thick. All of the films are aligned with the c -axis perpendicular to the surface.

X-ray absorption spectra were obtained at the Stanford Synchrotron Radiation Laboratory (beamline 4-3) using a Si(220) monochromator crystal. For each sample, several traces were collected at 80 K in fluorescence mode using a 13-element Ge detector. In each case, data were collected with the x-ray polarization vector approximately parallel or perpendicular to the film surface (within 9 degrees; the error in $\cos^2(\theta)$ is less than 3%) in order to probe different atoms within the structure. Count rates were kept below $5 \times 10^4/\text{sec}$ and corrected for the dead-time ($\sim 5 - 10 \mu\text{s}$) caused by the energy-resolving spectroscopy amplifier. An important use of the Ge detector was to remove Bragg spikes occurring at the incident beam energy in some of the channels. These spikes were removed by replacing them with the normalized average data for the other detector elements.

IV. EXPERIMENTAL RESULTS

A. Qualitative features

An example of the k -space data, $k\chi(k)$, for the four samples studied is shown in Fig. 2, with the polarization vector parallel to the c -axis. The Fourier Transform (FT) of these XAFS data is shown in Fig. 3a. Peaks in the r -space data correspond to neighbors at different distances with a phase shift, typically -0.4 to -0.2 Å, due to the photoelectron interaction with the potentials of both the absorbing and the neighboring atom. For these data, the first peak at ~ 1.4 Å corresponds to two O(4) neighbors along the c -axis, and is well ordered. However, the further neighbor peaks are very small in amplitude, much smaller than the corresponding peaks for Cu XAFS of an undoped high quality YBCO film. There should be large contributions from the Ba and Cu(2)/(Co(2)) neighbors in the 3-4 Å range; the absence of these well-defined peaks in the c -axis polarization data suggests a large amount of distortion and/or disorder in the Co further neighbors. This distortion/disorder appears to be similar for the three YBCO:Co samples but increases with Co concentration. In addition, the PBCO:Co sample also has a large distortion of the further neighbors even at only 5% Co.

The corresponding r -space plots for the ab -plane data are shown in Fig. 3b. Again, the first O peak (Co-O(1)/O(5)) is well defined (in this case it is an average within the ab -plane since the film is twinned and the amplitude is therefore reduced by a factor of two.) For this polarization, the further neighbor contributions in the 3-4 Å range should arise from the Ba and Cu(1)/Co(1) atoms.

A comparison of the data (Fig. 4) for the two orientations shows immediately (dotted lines in Fig. 4) that the c -axis and ab plane O atoms are at different distances by roughly 0.1 Å. This means that the Co is not in a cubic environment and the structure containing the Co is epitaxial with the substrate and the YBCO; hence, if Co were in a defect phase it would therefore have to be non-cubic and oriented with the substrate, which is unlikely. It is consistent with the Co replacing Cu in YBCO but with the CoO_z cluster displaced from the usual Cu(1) site. The c -axis O peak is primarily a Co(1)-O(4) peak (a Co(2)-O(4) bond length is expected to be much longer) and the fact that it is shorter than the Co-O(1) in the ab -plane supports the previous conclusion that Co substitutes primarily on the Cu(1) site. A comparison with c -axis polarized Cu K -edge pure YBCO film data (Fig. 4c; ab -plane data not shown) indicates that the Co-O peaks are shorter in both directions than the corresponding Cu-O peaks in the YBCO thin film; therefore, the O cluster about Co is contracted compared to that about Cu. In comparing the c -axis data note that for Co(1), there are two O(4) neighbors; for Cu there are 2/3 (1/3 of Cu is from Cu(1) \times 2 O(4) neighbors) at a distance of ~ 1.4 Å and 2/3 neighbors (2/3 of Cu is from Cu(1) \times 1 O(4) neighbor) at a longer distance of ~ 1.9 Å.

B. Comparison with data for powder samples

To compare the present results with earlier YBCO:Co powder XAFS data¹, the c -axis and ab -plane data for the thin films have been added together in the correct proportions ($2/3(ab\text{-plane}) + 1/3(c\text{-axis})$) to simulate a random orientation – i.e. a powder. (See Fig. 5 for a comparison of the resulting FT spectra.) There are similar Co concentrations for some of the YBCO:Co powder samples: for $x=0.07$ ($x = 0.08$ for powder) and for $x=0.10$ (same for powder). However there is no corresponding $x = 0.17$ powder sample. For this concentration, the film data seems most similar to the $x=0.30$ powder sample. The $x=0.05$ PBCO:Co data is more disordered in the further neighbors than YBCO:Co and also compares well with the $x=0.30$ powder data.

A comparison of the simulated powder data with our earlier powder data shows that the nearest neighbor oxygen environment around the cobalt is very similar in each case. For the further neighbors, the positions of the oscillations of the real part of the transform match well; however, the amplitude of the further neighbor peaks for the thin film and powder samples differ. Thus, the Co atoms appear to have similar distortions in powder and thin film samples, but the films show much more disorder. It is interesting to note that the 17% (film) data has the same amount of disorder as in a powder sample of nearly twice its concentration (in which most of the Cu(1) atoms have been replaced by Co) and supports the suggestion that Co forms clusters in the Cu(1) layer. This effect is even more pronounced in the 5% PBCO:Co film which has a comparable degree of disorder to that of the 30% powder sample. A large amount of disorder caused by such small concentrations of Co in the thin films may indicate larger Co clusters have formed in the 17% film which is similar to the structure when most of the Cu(1) is replaced by Co in the powder samples. The nature of the distortions and the amount of disorder are most likely sample dependent; however both the YBCO:Co and PBCO:Co films, which were grown in different laboratories, have more disorder at low Co concentrations than the corresponding bulk material. This might be evidence that the Co environment in thin film samples is inherently more disordered than in the bulk materials.

V. SIMULATED MODELS FOR POSSIBLE COBALT DISTORTIONS

The disorder and/or distortions in the further neighbors (Fig. 3) have so far proved too complicated to fit reliably. Therefore, we have calculated a number of theoretical XAFS simulations at a temperature of 80 K using the FEFF6 code^{21,22} in order to determine some possible distortions which might lead to the reduced further neighbor peaks. In these calculations, we first use the known crystal structure of YBCO to provide an approximately correct local geometry, and make separate calculations for Co on the Cu(1) and Cu(2) sites. This generates a simulation of the FT spectrum and provides a starting point for refinements of the local structure discussed below. If no distortions of the Co(1) or Co(2) sites occurred, the further neighbor peak amplitudes would be comparable to that observed for polarized Cu K -edge studies of pure YBCO thin films. As noted above, this is inconsistent with the data (see Fig. 4c). We next consider several possible distortions for Co on the Cu(1) site. First, we use the distortions obtained in earlier studies^{1,11} of bulk powder samples which suggested that a fraction of the Co are displaced off-center along the $\langle 110 \rangle$ direction by $\sim 0.2 \text{ \AA}$; the fraction depended on the type of Co chain-like clusters that formed. We also include a small contraction of both nearest neighbor Co-O bond distances. Using typical Debye-Waller parameters, the Co further neighbor composite-peak for this distorted site are significantly larger than observed in the film data. For the c -axis data, the simulations show that the Co(1)-Ba peak is considerably reduced, but a large Co(1)-Cu(2) peak (which includes multi-scattering from Co(1)-O(4)-Cu(2)) occurs near 3.7 \AA in the r -space data, that is not significantly decreased by this ab -plane distortion. Consequently, to explain the lack of such a peak in the c -axis data, requires that some other distortion/disorder be present. The O(4) atoms may be displaced such that the Co(1)-O(4)-Cu(2) unit is not co-linear, thus reducing the multi-scattering contribution²⁰, or the Co might be displaced along the c -axis. We could alternatively use a large Debye-Waller parameter, σ ; to suppress the Co-Cu(2) peak sufficiently would require $\sigma \sim 0.1 \text{ \AA}$.

For the first type of distortion, with the Co displaced $\sim 0.2 \text{ \AA}$ in the $\langle 110 \rangle$ direction, perfect co-linearity would require the O(4) to be displaced $\sim 0.1 \text{ \AA}$ in the $\langle 110 \rangle$ direction. However, the difference in the simulation between perfect co-linearity and an undisplaced O(4) is small. We then consider a number of O(4) displacements (eg. $0, 0.1, 0.2 \text{ \AA}$) in the $\langle \bar{1}10 \rangle$ direction to further decrease the multi-scattering contribution. The O(4) atoms must be displaced in this way by $\sim 0.2 \text{ \AA}$ (Fig. 6a) from its original site in order to have an amplitude of the Co(1)-Cu(2) peak comparable to what is found experimentally. It is not clear what would drive such a distortion in this crystal.

If the Co were distorted only along the c -axis, the Co-Ba would still be visible, although slightly reduced in amplitude, as shown in Fig. 6b (the Co-Ba contribution has a peak near 3.3 \AA). Such a distortion would produce two Co-Cu(2) peaks which could destructively interfere. To reduce the Co(1)-Cu(2) peak amplitude (at 3.7 \AA) in this way to be comparable with the thin film data would require a displacement of the Co by $\sim 0.1 \text{ \AA}$. In order to reduce both the Ba and Cu(2) peaks, a combination of the above Co displacements (both in the $\langle 110 \rangle$ and $\langle 001 \rangle$ directions) may be necessary. In Fig. 6c we show simulations with the Co displaced $\sim 0.2 \text{ \AA}$ in the $\langle 110 \rangle$ direction as before, but with a variety of displacements (eg. $0, 0.05, \text{ and } 0.10 \text{ \AA}$) in the $\langle 001 \rangle$ direction as well.

The argument presented previously for a $\langle 110 \rangle$ Co distortion is based on the contracted Co-O bond length in the ab -plane. If the two nearest O neighbors are on the a and b axes, the short Co-O bonds support the conclusion that the Co atoms have a $\langle 110 \rangle$ off-center displacement. The possibility of a c -axis displacement is less clear. Since the CoO_z cluster is contracted, it may be that the cluster is unstable on the Cu(1) site and moves towards one of the neighboring Cu(2) atoms.

Finally, we note that simulations for the ab -plane data show that a $\langle 110 \rangle$ Co distortion reduces both the Co(1)-Ba and the Co-Cu(1)/Co(1) contributions, but for a $\sim 0.2 \text{ \AA}$ distortion, the suppression is not as large as observed in the film data. c -axis displacements will reduce the Co(1)-Ba neighbor peak further but not the Co-Cu(1)/Co(1) peak.

VI. DETAILED FITS AND DISCUSSION

For detailed fits of the data we used theoretical standard functions for the various atom-pairs (Co-O, Co-Ba etc.) calculated using the FEFF6 code. In our previous study^{1,11} of YBCO:Co bulk samples, we proposed that the cobalt ions formed short zigzag chains along the $\langle 110 \rangle$ direction in the Cu(1) layer. $\langle 110 \rangle$ displacements of some of the Co could produce a long Co-O peak (at 2.4 \AA), 3 Ba peaks, one at the normal distance and two separated by $+\text{ or } -\delta r$ from it, and a shortened Co-Cu(1)/Co. Full fits to the nearest neighbors out to 4 \AA to both the ab -plane and c -axis orientations using this distortion were tried as well as to other distortion models (such as Co displaced a fixed amount in the $\langle 110 \rangle$ and then distorted along the $\langle 001 \rangle$ direction, or Co displaced in the $\langle 100 \rangle$ direction, etc.) all with similar results: fits to the further neighbors were of poor quality. Thus, we have limited our fits to only the first neighbor O atoms.

For the c -axis data, we used a FT range of $4.5\text{-}11.5 \text{ \AA}^{-1}$ and only fit the first neighbor O peak, either to a single peak or to a sum of two peaks. Generally the single peak fit (r -space fit range $1.2\text{-}1.8 \text{ \AA}$) was good, but there were a couple discrepancies – the Debye Waller parameter was too small in some cases and the deviation between the fit and the data was worse near the higher part of the fit range. The single peak fit results are summarized in Table I and the fits to the Co-O(4) peak are shown in Fig. 7a. The O(4) distribution is consistently short at a distance of $\sim 1.80 \text{ \AA}$ (YBCO has a Cu(1)-O(4) bond length of 1.86 \AA). For the two peak fit we extended the r -space fit range slightly to $1.2\text{-}2.0 \text{ \AA}$, and obtained a significantly better fit (this fit matched the main part of the r -space peak better); however, the second peak which occurs at a longer distance of $\sim 2.3 \text{ \AA}$ has a small amplitude of perhaps 20%. This longer O(4) peak might be consistent with a Co(2)-O(4) bond. However, since the second peak in the fits overlaps the tail of the Co-Ba peaks it is not clear that this O peak is significant.

For the ab -plane data, the highest quality fits to the Co-O(1) distribution (Fig. 7b) were obtained using a k -window of $3.5\text{-}11.5 \text{ \AA}^{-1}$ and a fit range of 1.2 to 1.8 \AA . This peak is well ordered, although for the $x=0.07$ sample a one peak distribution does not fit well. Another peak at $\sim 2.3 \text{ \AA}$ improves the quality of the fit but without a reasonable fit to the further neighbors, it is difficult to conclude at the present time whether this peak is real or if it is only correcting in a crude way for the tail of the further neighbor peaks.

Our results of short, well-defined Co-O peaks, yet disordered further neighbors, for both the c -axis and ab -plane YBCO:Co and PBCO:Co data indicate the presence of CoO_z clusters. The average distance of this first neighbor shell is 1.83 \AA ($1/2 \times 1.79 + 1/2 \times 1.86 = 1.83 \text{ \AA}$) and increases slightly with increasing Co concentration. If it is assumed that Co has an overall reduction factor, S_o^2 , of 0.7, then there are ~ 2 O(4) and $\sim 2\text{-}3$ O(1) neighbors. These results are very similar to those found in previous measurements on YBCO:Co powders^{1,9,11}. The reduced amplitude of the Co-Ba and Co-Cu(1)/Cu(2) peaks observed in our data is indicative of Co(1) being displaced from the (000) position rather than just some other distortion in these atom pairs, although both situations are possible. Off-center distortions of the Co atoms are consistent with our earlier work^{1,11} as well as that of Renevier *et al.*^{9,23}, but in disagreement with others who found no distortions^{8,24}.

VII. CONCLUSION

We have investigated the local structure about Co in YBCO:Co and PBCO:Co thin films and compared our results with measurements on bulk powder samples. The nearest neighbor oxygen atoms are well ordered in both data sets which is evidence of the formation of tightly bound CoO_z clusters. The Co-O distances along the c -axis and within the ab -plane are distinctly different and shortened compared to similar Cu-O bonds in YBCO in both cases: 1.80 and 1.88 \AA respectively. Thus, the Co substitutes in a region that is epitaxial with the c -axis oriented YBCO. The short Co-O bond distance for the c -axis polarization supports the Co(1) substitution site, but a small fraction, up to 10-20%, may be on the Cu(2) site. The further neighbors peaks are decreased in amplitude in the films relative to powder samples, indicating that the Co environment in these films is more disordered or distorted than in the powder samples. Theoretical simulations suggest that the Co could be distorted along the $\langle 001 \rangle$ direction in addition to a distortion in the $\langle 110 \rangle$ direction; alternatively, the suppression of the Co(1)-Cu(2) peak requires a large Debye-Waller factor of $\sim 0.1 \text{ \AA}$. This would produce the decreased amplitude observed in the data, but we are unable to determine the exact nature of the distortion at the present time.

ACKNOWLEDGMENTS

The experiments were performed at the Stanford Synchrotron Radiation Laboratory, which is operated by the U.S. Department of Energy, Division of Chemical Sciences, and by the NIH, Biomedical Resource Technology Program, Division of Research Resources. The work is supported in part by NSF grant DMR-92-05204.

¹ F. Bridges, J. B. Boyce, T. Claeson, T. H. Geballe, and J. M. Tarascon, Phys. Rev. B **39**, 11603 (1989).

² M. Kakihana, L. Börjesson, and S. G. Eriksson, Physica B **165**, 1245 (1990).

³ M. Kakihana, S.-G. Eriksson, L. Börjesson, L.-G. Johansson, C. Ström, and M. Käll, Phys. Rev. B **47**, 5359 (1993).

⁴ B. Moeckly and K. Char (unpublished).

⁵ B. Zhao, Y. Shi, Y. Zhao, and L. Li, Phys. Rev. B **38**, 2486 (1988).

- ⁶ F. Bridges, J. B. Boyce, and R. I. Johnson, *App. Phys. Lett.* **60**, 3042 (1992).
- ⁷ P. Zolliker, D. Cox, J. Tranquada, and G. Shirane, *Phys. Rev. B* **38**, 6575 (1988).
- ⁸ C. Y. Yang, A. R. Moodenbaugh, Y. L. Wang, Y. Xu, S. M. Heald, D. O. Welch, M. Suenaga, D. A. Fischer, and J. E. Penner-Hahn, *Phys. Rev. B* **42**, 2231 (1990).
- ⁹ H. Renevier, J. L. Hodeau, M. Marezio, A. Fontaine, A. Michalowicz, and G. Tourillon, *Phys. Rev. B* **47**, 1398 (1993).
- ¹⁰ C. Blue, K. Elgaid, I. Zitkovsky, P. Boolchand, D. McDaniel, W. C. H. Joiner, J. Oostens, and W. Huff, *Phys. Rev. B* **37**, 5905 (1988).
- ¹¹ G. G. Li, F. Bridges, J. B. Boyce, and W. C. H. Joiner, *Phys. Rev. B* **47**, 12110 (1993).
- ¹² H. Renevier, J. L. Hodeau, M. Marezio, M. Bessière, E. Elkaim, and S. Lefèbvre, *Physica C* **230**, 31 (1994).
- ¹³ H. Renevier, J. L. Hodeau, M. Marezio, and A. Santoro, *Physica C* **220**, 143 (1994).
- ¹⁴ J. W. Martin, G. J. Russell, D. D. Cohen, and A. Hartmann, *Physica C* **247**, 34 (1995).
- ¹⁵ K. Char, L. Antognazza, and T. H. Geballe, *Appl. Phys. Lett.* **65**, 904 (1994).
- ¹⁶ L. Antognazza, S. J. Berkowitz, T. H. Geballe, and K. Char, *Phys. Rev. B* **51**, 8560 (1994).
- ¹⁷ G. Koren and E. Polturak, *Physica C* **230**, 340 (1994).
- ¹⁸ L. W. Song, E. Narumi, F. Yang, H. Shao, and Y. H. Kao, *Physica C* **174**, 303 (1991).
- ¹⁹ T. M. Hayes and J. B. Boyce, in *Solid State Physics*, edited by H. Ehrenreich, F. Seitz, and D. Turnbull (Academic, New York, 1982), Vol. 37, p. 173.
- ²⁰ B. K. Teo, *EXAFS: Basic Principles and Data Analysis* (Springer-Verlag, New York, 1986).
- ²¹ J. J. Rehr, R. C. Albers, and S. I. Zabinsky, *Phys. Rev. Lett.* **69**, 3397 (1992).
- ²² S. I. Zabinsky, A. Ankudinov, J. J. Rehr, and R. C. Albers, *Phys. Rev. B* **52**, 2995 (1995).
- ²³ H. Renevier, X. B. Kan, J. P. Quintana, and J. B. Cohen, *J. Mater. Res.* **9**, 3050 (1994).
- ²⁴ B. D. Padalia, S. Gurman, P. Mehta, and O. Prakash, *J. Phys. Condens. Matter* **4**, 6865 (1992).
- ²⁵ R. P. Sharma, F. J. Rorella, J. D. Jorgensen, and L. E. Rehn, *Physica C* **174**, 409 (1991).

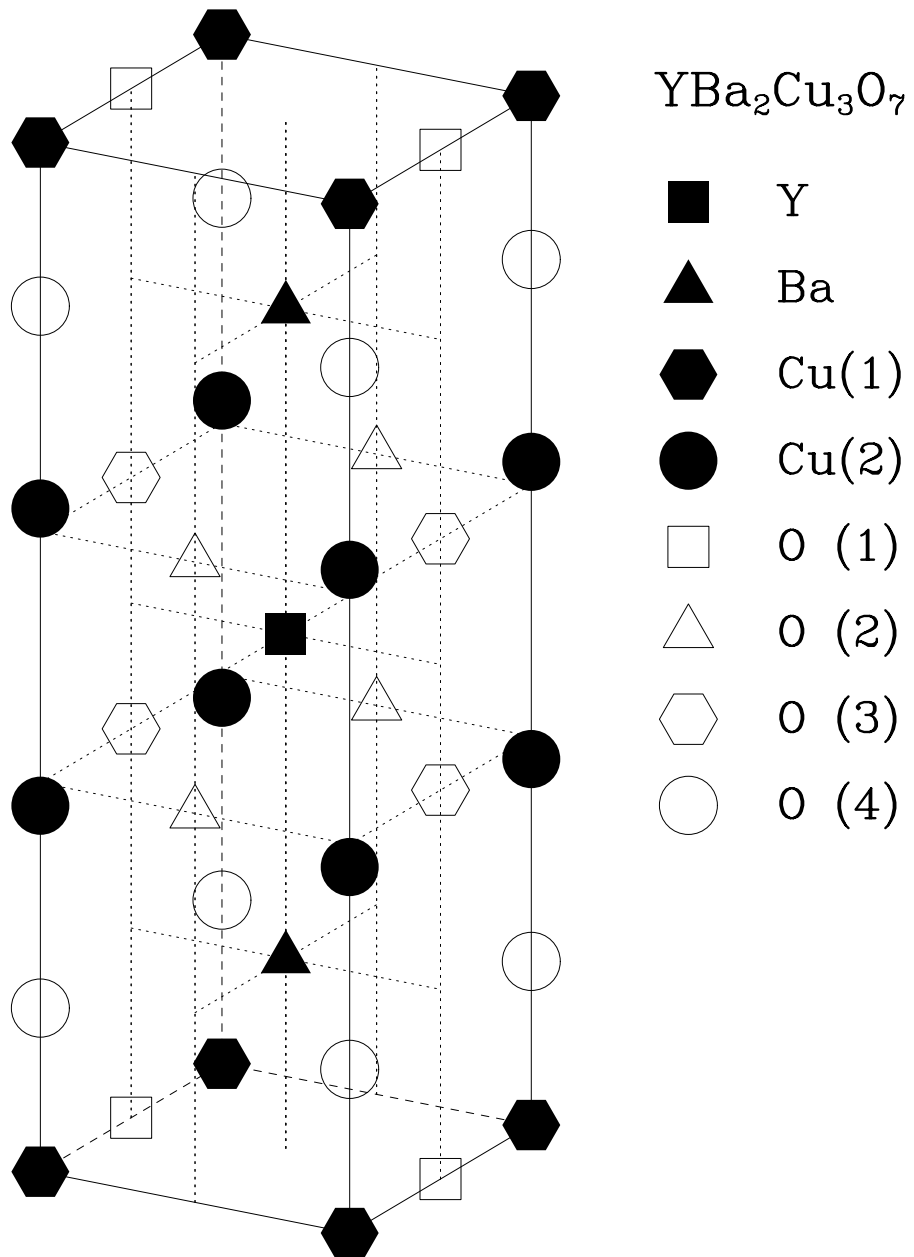


FIG. 1. The crystal structure for $\text{YBa}_2\text{Cu}_3\text{O}_{7-\delta}$. Co is thought to substitute primarily on the Cu(1) site. The O(5) site (not shown) lies halfway in between the Cu(1) sites along the a -axis.

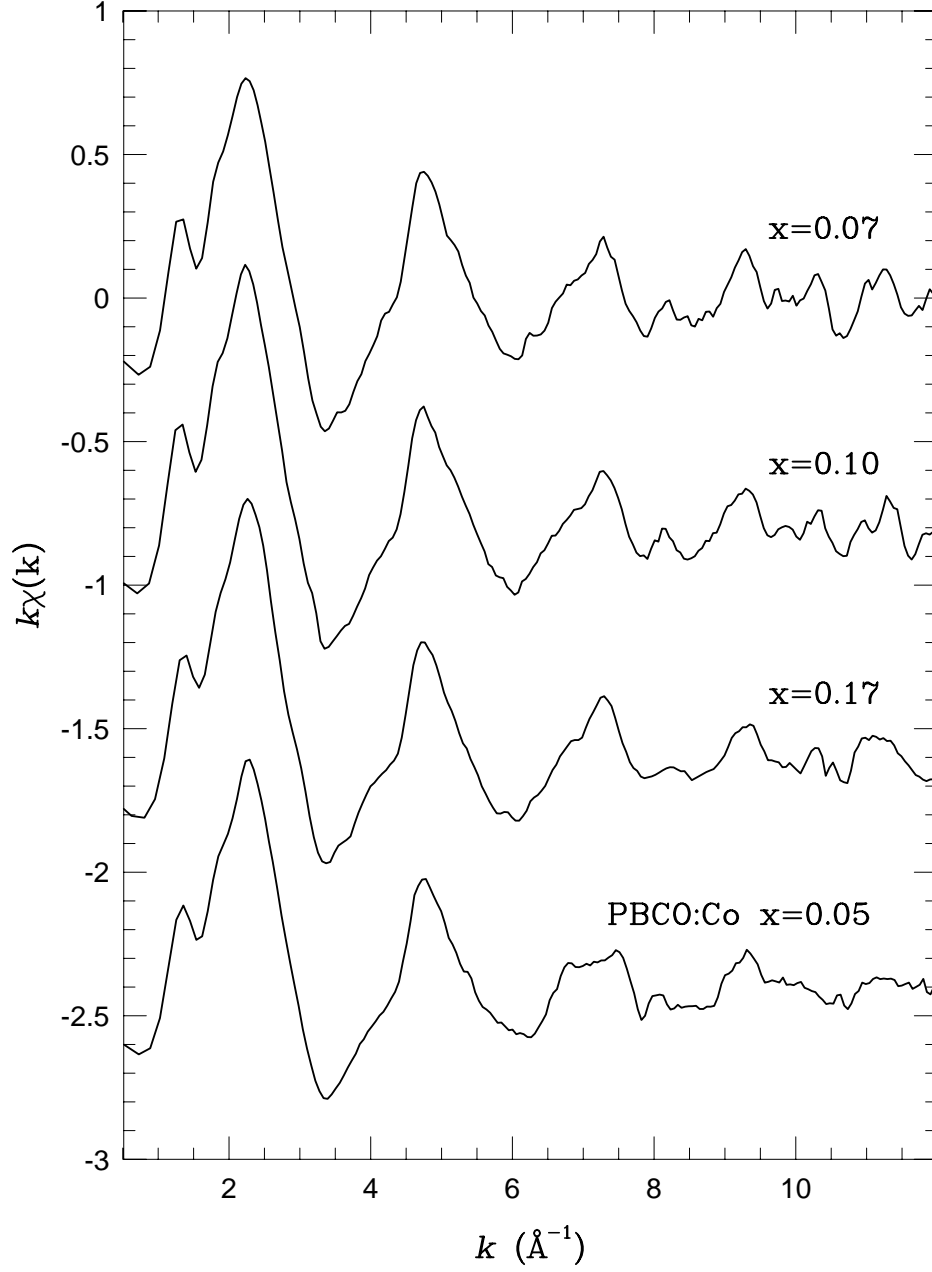


FIG. 2. $k\chi(k)$ vs. k for the Co K -edge with the polarization along the c -axis for the three concentrations of $\text{YBa}_2(\text{Cu}_{1-x}\text{Co}_x)_3\text{O}_{7-\delta}$ and the $\text{PrBa}_2(\text{Cu}_{1-x}\text{Co}_x)_3\text{O}_{7-\delta}$ sample. The three curves below the top one have been displaced for clarity.

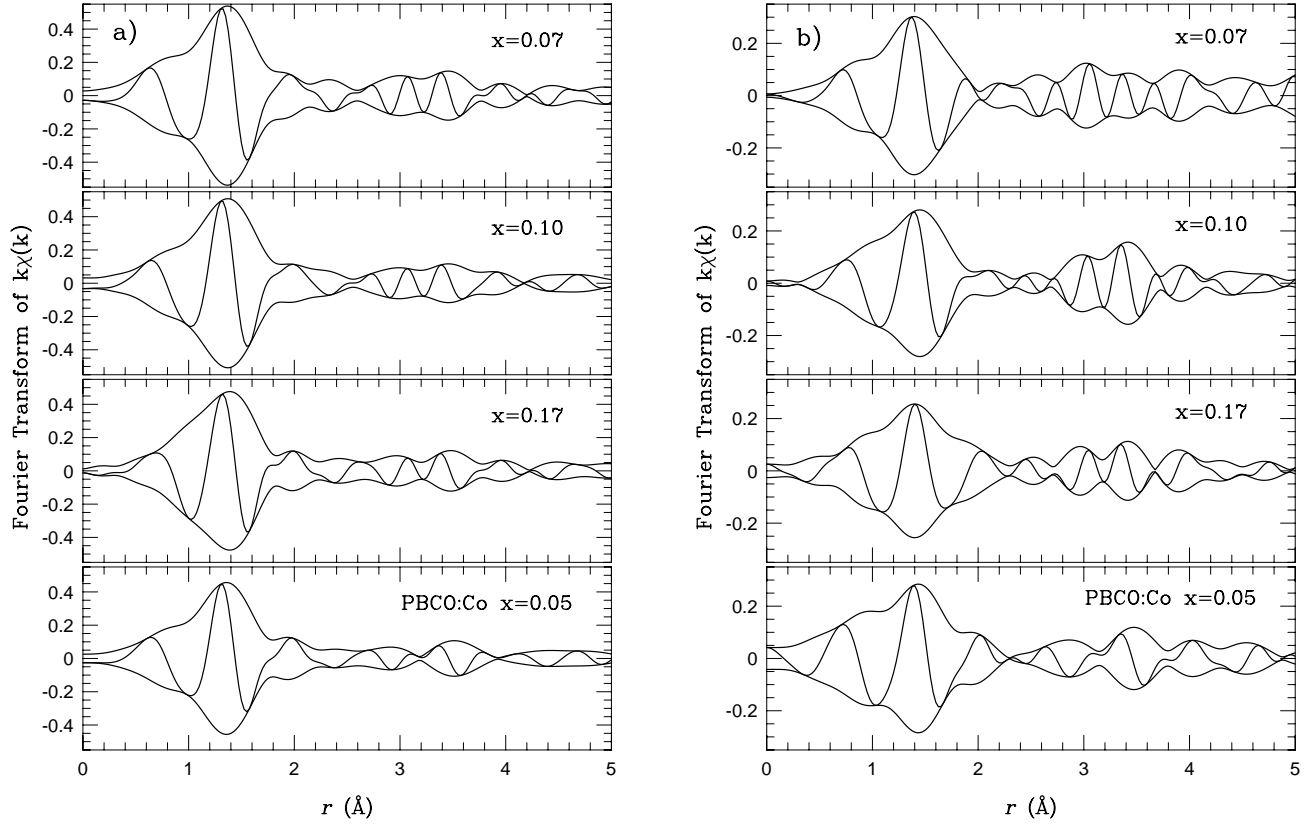


FIG. 3. The left panel a) is the Fourier Transform of the c -axis Co K -edge data for the three YBCO:Co concentrations with the PBCO:Co data on the bottom. The right panel b) shows the Fourier Transform of the ab -plane data for the same samples. The envelope curves are the magnitude of the transforms and the fast oscillatory curves are the real parts of the transforms. For each data set the transform range is from 3.5 to 11.5 \AA^{-1} and Gaussian broadened by 0.3 \AA^{-1} .

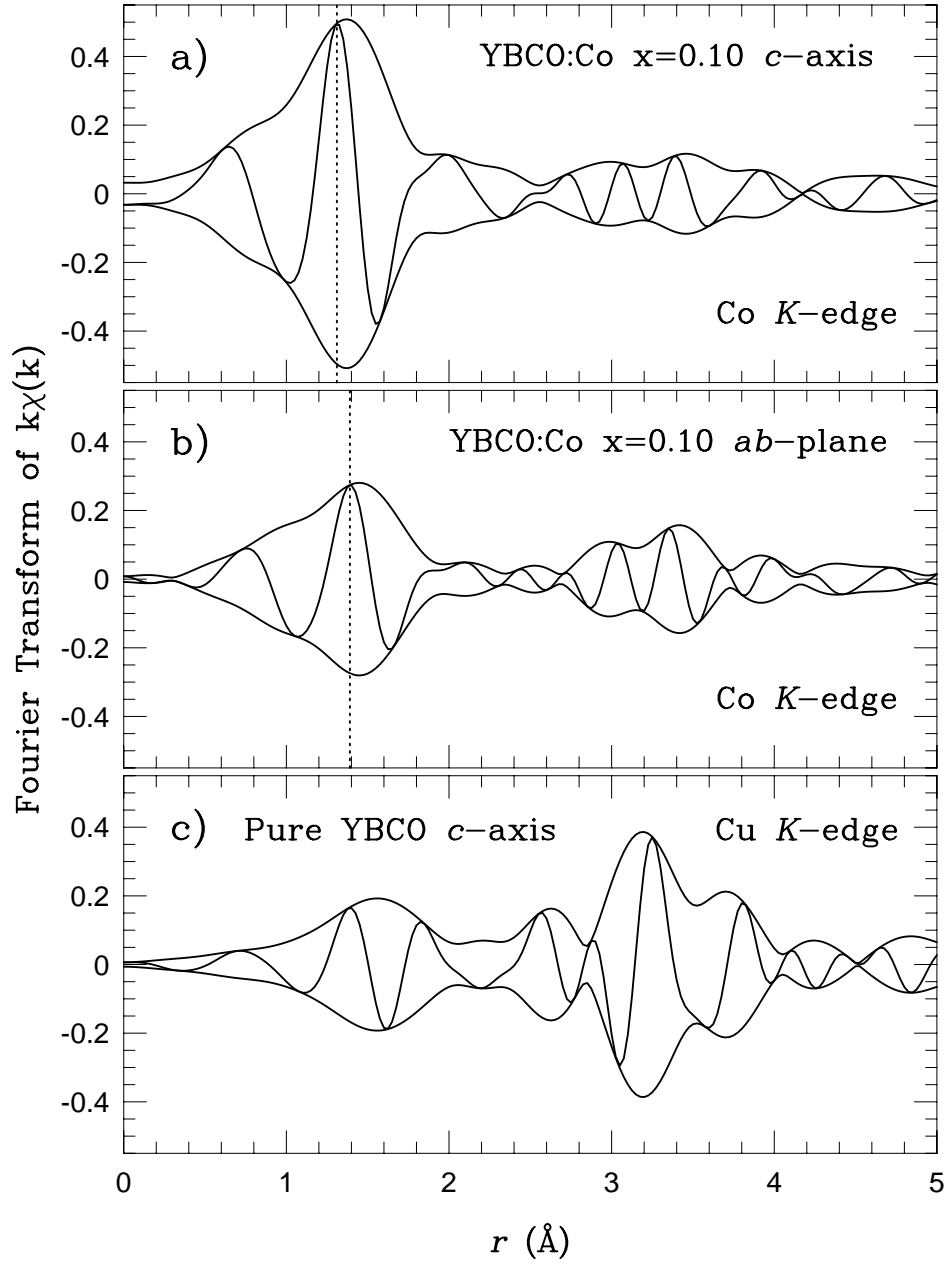


FIG. 4. A comparison of the YBCO:Co with $x=0.10$ of the a) c -axis Co K -edge data and the b) ab -plane Co K -edge data. c -axis polarized Cu K -edge data from normal YBCO is shown in c). For each data set the transform range is from 3.5 to 11.5\AA^{-1} and Gaussian broadened by 0.3\AA^{-1} .

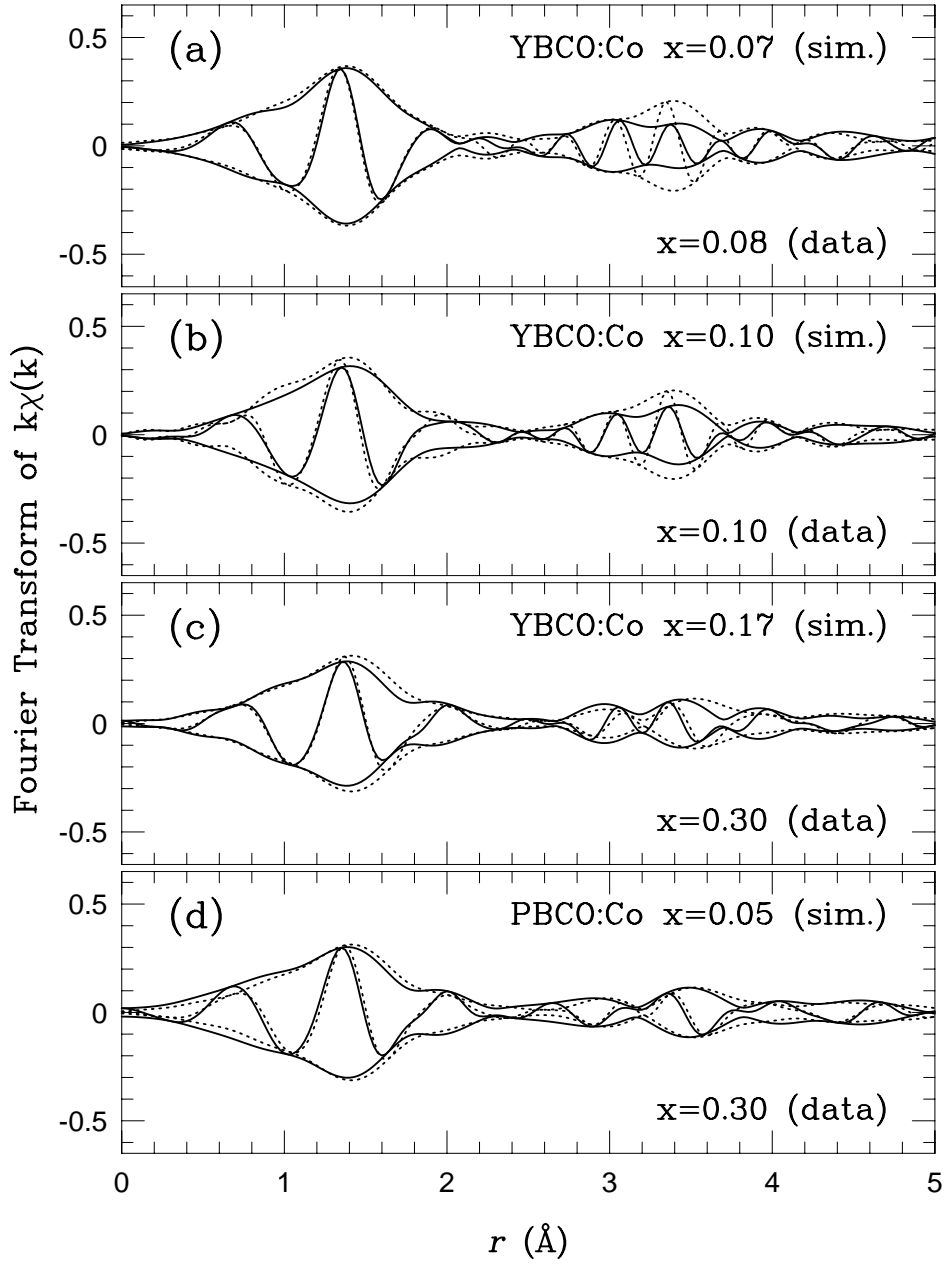


FIG. 5. a) Comparison of YBCO:Co with $x=0.07$ c -axis and ab -plane Co K -edge data added together in the proportions $2/3(ab\text{-plane}) + 1/3(c\text{-axis})$ (solid) to that of an 8% powder sample (dotted); b) summed 10% film data (solid) and 10% powder data (dotted); c) summed 17% film data (solid) and 30% powder data (dotted); d) the summed PBCO:Co film data (solid) is most similar to the 30% powder data (dotted). For all panels, the k -window is 3.5 to 11.5 \AA^{-1} and Gaussian broadened by 0.3 \AA^{-1} .

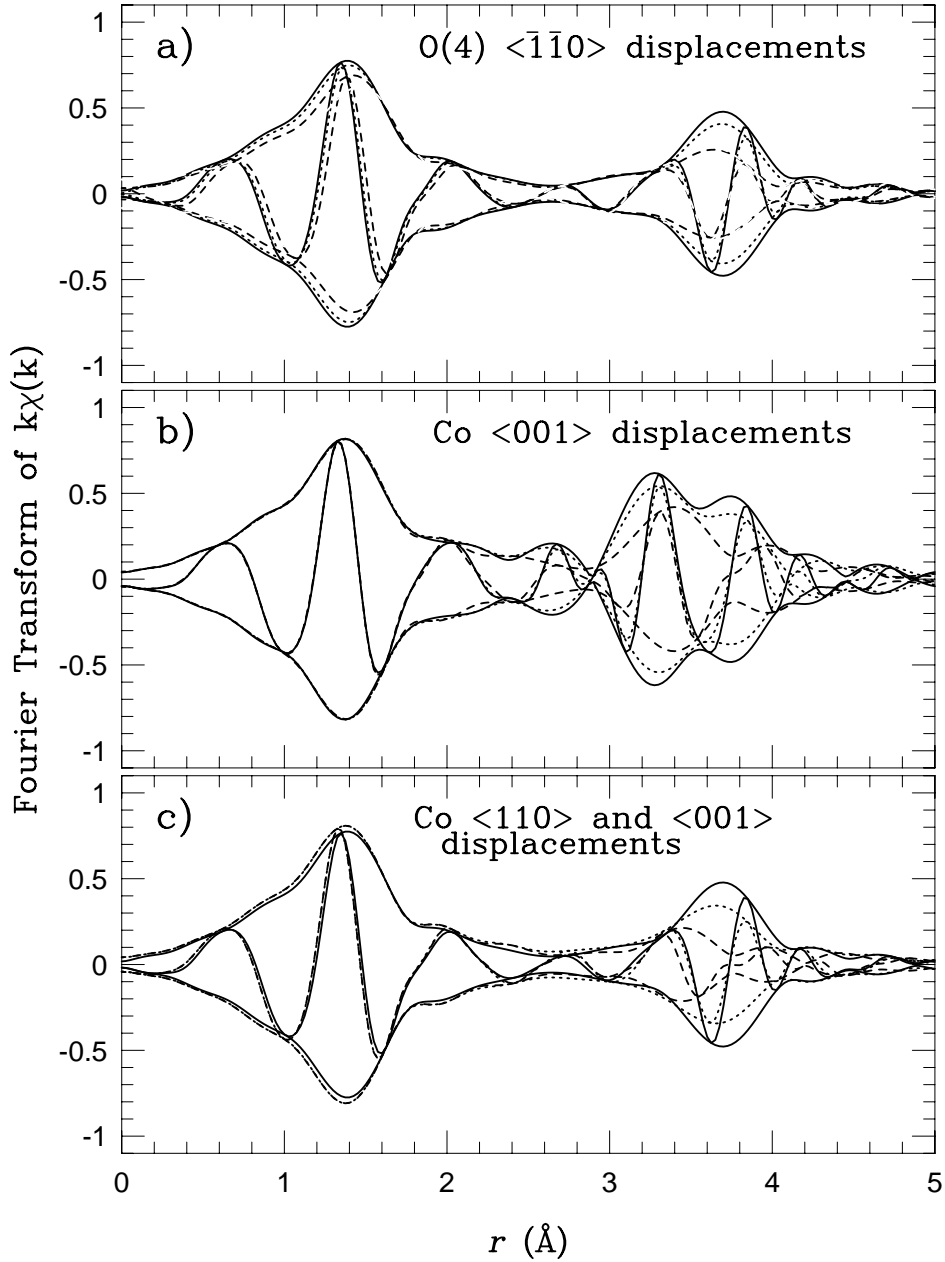


FIG. 6. FEFF simulations at $T=80$ K for the Co K -edge with polarization vector along the c -axis. a) illustrates various O(4) displacements: O(4) not moved from its original site (solid), O(4) displaced by 0.1 Å (dotted), and O(4) displaced by 0.2 Å (dashed) in the $\langle \bar{1}\bar{1}0 \rangle$ direction. The Co(1) atom is distorted by 0.2 Å in the $\langle 110 \rangle$ direction in each case. b) shows simulations of various displacements of the Co(1) along the $\langle 001 \rangle$ direction: Co(1) in the ideal Cu(1) site (solid), and Co(1) displaced by 0.05 Å (dotted) and 0.10 Å (dashed). c) shows simulations in which the Co(1) atom is displaced 0.2 Å in the $\langle 110 \rangle$ direction (solid) as in a) but with an additional displacement along the c -axis: Co(1) displaced by 0.05 Å (dotted) and 0.10 Å (dashed). In the last two panels, the Co-O(4) distances have been shortened by 0.05 Å for a better simulation of the film data. For each data set the transform range is from 3.5 to 11.5 Å $^{-1}$.

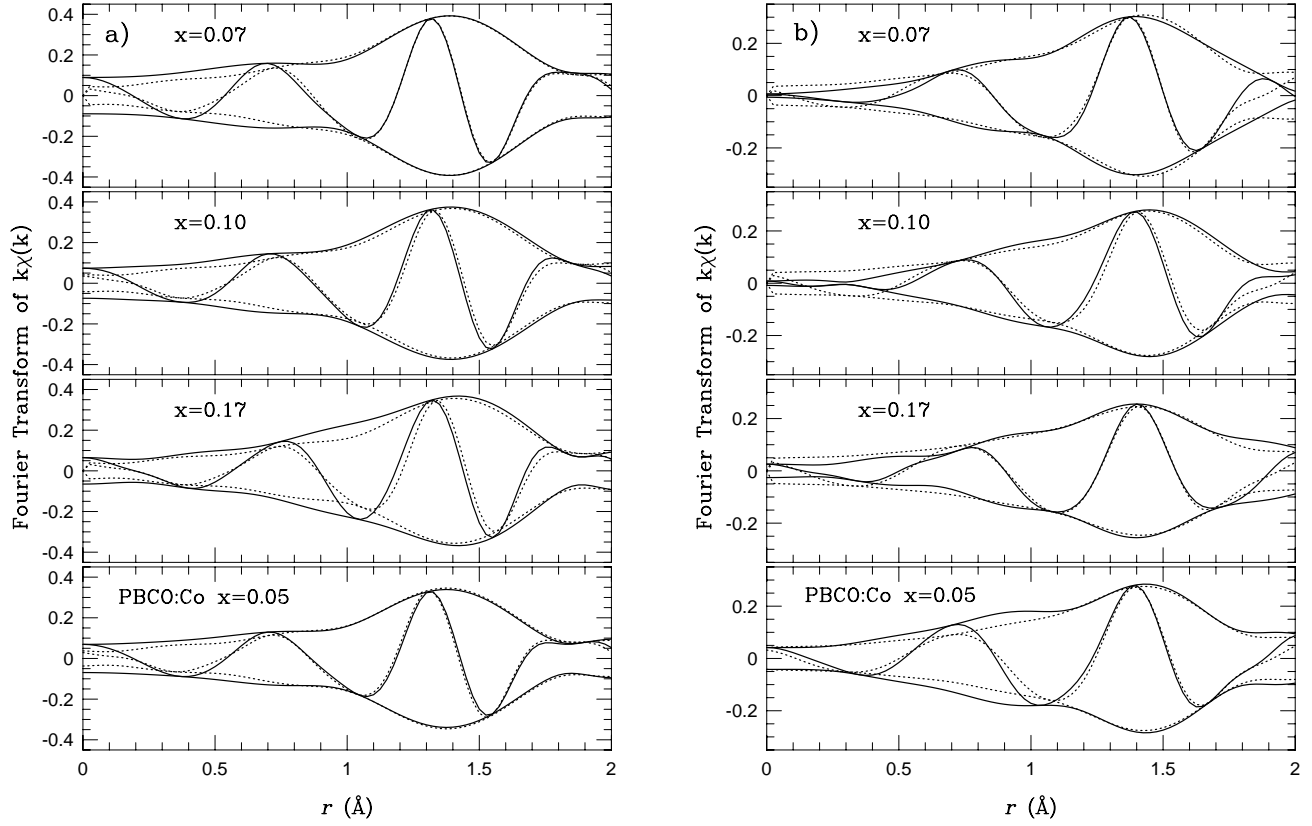


FIG. 7. a) single peak fits (dotted) to the Co-O(4) atom-pair for the c -axis data (solid). The fit range is from 1.2 to 1.8 Å. The k -window for the fits is 4.5 to 11.5 Å⁻¹ and Gaussian broadened by 0.3 Å⁻¹. b) single peak fits (dotted) to the Co-O(1) atom-pair for the ab -plane data (solid). The fit range is from 1.2 to 1.8 Å. The k -window for the fits is 3.5 to 11.5 Å⁻¹ and Gaussian broadened by 0.3 Å⁻¹.

TABLE I. Single peak fit results of the nearest neighbor oxygen atoms for both the c -axis and ab -plane YBCO:Co and PBCO:Co thin film Co K -edge data. The uncertainties in measurements were estimated to be 0.02 \AA for bond lengths, R , and 0.005 \AA for the Debye-Waller parameter, σ . The amplitude reduction factor, S_0^2 , has an average value of 0.7. The Cu(1)/Co(1)-O bond lengths should be selected appropriately: Cu(1) for YBCO and Co(1) for YBCO:Co or PBCO:Co.

	YBCO		YBCO:Co		PBCO:Co
Concentration, x	0	0.07	0.10	0.17	0.05
R (Cu(1)/Co(1)-O(4)) [\AA]	1.8597 ^a	1.79	1.80	1.83	1.78
R (Cu(1)/Co(1)-O(1)) [\AA]	1.9407 ^a	1.86	1.88	1.88	1.87
σ (Co(1)-O(4)) [\AA]		0.049	0.058	0.048	0.040
σ (Co(1)-O(1)) [\AA]		0.041	0.041	0.069	0.056

^a Neutron diffraction results at $T=80 \text{ K}$ from Sharma *et al.*²⁵